

Pipe vs. Shell Finite Element Modeling of CANDU Feeders

Usama Abdelsalam⁽¹⁾, DK Vijay⁽²⁾

¹Senior Engineer, Nuclear Safety Solutions Ltd., Toronto, Ontario

²Section Manager, Nuclear Safety Solutions Ltd., Toronto, Ontario, Canada

ABSTRACT

The stress index, C_2 , and flexibility factor, k , are used in piping computer programs to handle bends/elbows using straight beam formulations. The ASME code Section III NB-3600 (Piping Design) equation for the C_2 stress index is known to be conservative in order to cover a wide range of bends/elbows. As per the ASME code equations, neither of these factors takes into consideration the bend angle nor bend-to-bend connections whether in-plane or out-of-plane. To reduce the conservatism in fitness for service analyses, the finite element method is used to calculate more specific values for the stress index that fit the problem at hand. In this paper, detailed FEA analyses using 3D shell elements are performed to calculate reduced C_2 values. Piping analyses are conducted using the FEA calculated stress indices to explore the accuracy of the pipe element approach using FEA calculated stress indices as compared to a 3D shell model approach. The comparison is based on the modal allowable vibration velocities for CANDU feeder piping calculated using ASME OM S/G-2003. In addition, the seismic response under Seismic Anchor Movements (SAM) and Frequency Response Spectrum loadings (FRS) is also considered for the comparison. The results of the analyses showed that the use of the FEA calculated stress index along with the ASME code flexibility factor is not conservative compared to the results obtained from full 3D shell models. The results also show that the use of the ASME code case N-319-3 to calculate a reduced flexibility improves the accuracy; however, the results are still on the non-conservative side compared to the shell model results. It is the purpose of this paper to show that the stress index, C_2 , and flexibility factor, k , should be treated as a conjugate pair.

INTRODUCTION

In a typical CANDU reactor, 480 fuel channels are arranged horizontally in a lattice inside the Calandria Vessel. The nuclear fuel bundles are placed inside the Fuel Channels (FC). The heavy water flowing in the fuel channels transports the heat energy generated from the nuclear reaction to the steam generators. The flow of the heavy water coolant through the fuel channels is provided by four Primary Heat Transport (PHT) pumps and carried through pipes running from the inlet headers and removed through pipes connecting to the outlet header. Each fuel channel is connected to two pipes called inlet and outlet feeders, respectively. CANDU feeders are made of Low Carbon Steel SA-106 Gr. B pipes with tight radius bends/elbows welded to the Grayloc hub that is assembled to the end-fittings at the ends of the fuel channels. The pipe sizes used are in the 2-3.5" outer diameter range with thickness in the 0.218-0.3" range.

It is observed that the outlet feeders may encounter considerable wall thinning due to the flow accelerated corrosion (FAC) phenomenon. The wall thinning is more pronounced at the tight radius elbow/bend regions close to the Grayloc hub that connect the feeder lower end to the end-fitting of the fuel channel. The reduced wall thickness leads to higher stresses that need to be assessed to demonstrate feeders' fitness for continued service. Feeders in CANDU nuclear reactors are part of the Primary Heat Transport system (PHT) and are classified as Class 1 piping components. Therefore, CANDU feeders were designed according to ASME PVP Code Section III Subsection NB-3600 (Piping Design).

During planned outages for CANDU reactors, fuel bundles may be removed from selected fuel channels for inspection and other maintenance purposes. The preferred method of removing the fuel bundles from the fuel channels is flow de-fuelling. In the flow de-fuelling operation, the latches that prevent the fuel bundles from moving out from their locations inside the fuel channel are opened allowing them to move out to the fuelling machine. The flow rate inside the channel increases due to the reduced flow resistance as the fuel bundles clear out of the channel. This increased flow rate may cause the feeders to vibrate at higher than normal vibration levels and thus become susceptible to fatigue failure. To assess the integrity of feeders during the flow de-fueling operation, a velocity criterion based on the alternating stress limit as per ASME OM S/G-2003 1 is used. In the velocity criterion the maximum feeder vibration velocity is compared to the allowable for the feeder. A feeder passes the velocity criterion if the calculated allowable vibration velocity is larger than the maximum feeder vibration velocity.

The ASME O&M reference the ASME Section III - NB3600 for the calculation of the secondary stress indices 2. It is noted that ASME OM-S/G-2003 Part 3 addresses the pre-operational and initial start-up vibrations. However, the scope suggests that it "may also serve as a guide to assess vibration levels of applicable piping systems during plant operation". The vibration velocity criterion covers the steady state vibrations of feeder piping classified as "Vibration Monitoring Group 1" (VMG 1). As per section 3.2.1.2 of the OM standards (VMG 1), the maximum calculated alternating stress intensity S_{alt} is limited by:

$$S_{alt} = \frac{C_2 K_2}{Z} M \leq \frac{S_{el}}{\alpha}$$

Where,

- C_2, K_2 = Secondary and Peak Stress Indices as defined in ASME BPV Code, Section III NB-3600
- M = Maximum zero to peak dynamic moment loading
- S_{el} = $0.8 S_A$, where S_A is the alternating stress at 10^6 cycles in psi from ASME BPV Code, Section III, Fig. 1-9.1
- Z = Section modulus of the pipe
- α = allowable stress reduction factor (1.3 for materials covered by ASME BPV Code, Section III, Fig. 1-9.1)

Assuming that each feeder may vibrate at each natural mode within the frequency range of interest (0-180HZ), the following vibration velocity criterion is applied:

$$V_{all} \geq V_{max} \quad \rightarrow \text{Velocity Criterion}$$

where,

- V_{all} = Calculated Allowable vibration velocity derived from the allowable alternating stress
= $V_{mmax} * S_{alt}/S_{mmax}$
- V_{mmax} = Maximum modal velocity
= $2\pi * f * U_{mmax,i}$
- U_{mmax} = Maximum modal Displacement
- S_{mmax} = Maximum modal stress intensity
- V_{max} = Maximum vibration velocity

The calculated allowable velocity is conservatively taken as the minimum allowable considering all natural modes within the 0-180 HZ frequency range.

Commercial piping codes are used to perform the piping stress analyses using the finite element method adopting beam-like pipe elements. To account for the stress intensification and flexibility effects at curved pipe segments, special ASME formulas are used as per NB-3680 addressing stress indices and flexibility factors. NB-3683.7 provides the equation for the secondary stress index while NB-3686.2 provides the equation for the calculation of the flexibility factor for curved pipe and welding elbows. These Code formulas are conservative to accommodate a wide range of piping sizes and layouts.

Three main stress indices used are B-indices based on limit load type of analysis, C-indices representing the Primary-plus-Secondary stresses and K-indices representing peak stresses that are involved in fatigue calculations. Matzen and Tan 3 provide a quite interesting discussion of the history of the stress indices with an elaborate list of references.

In fitness for service analyses, it is desired to reduce the level of conservatism by deriving factors that are specific to the problem at hand. Eom et. al discussed the level of conservatism when three ASME specified indices are used at an elbow to elbow weld connection 4. Tan and et. al 5 proposed a new design equation for the B2 index based on finite element analysis. Matzen and Tan 6 published a report summarizing the results obtained from their finite element analyses to calculate the B2 index along with supporting experimental test results. Saleem & Kumar 7 presented a methodology to calculate a finite element based secondary stress index. It was shown that the secondary stress index is dependent on the bend/elbow angle and confirmed the embedded conservatism in the ASME code formulas 8.

The secondary stress index, C_2 , is only used as a post-processing operator in piping programs to magnify the stresses after the solution; i.e., it does not affect the stiffness or flexibility of the pipe (beam) elements. Higher stress indices result in higher stresses. Therefore, lower FEA calculated stress indices produce lower stresses leading to reduced conservatism in the stress calculations. To draw a similar statement on the flexibility factors is a bit more involved. The flexibility factor comes into play when the bending moment of inertia is calculated during the stiffness matrix formation. The moment of inertia for bends is calculated by dividing the moment of inertia of the section by the flexibility factor, k , as follows [9]:

$$I = \frac{\pi (D_o^4 - D_i^4)}{64 k},$$

where, D_o , and D_i are the pipe outer and inner diameters, respectively, and k is the flexibility factor. The flexibility factor is 1 for straight pipes and it increases as the bend angle increases. As the bend angle decreases, the flexibility decreases approaching the straight pipe flexibility. Lower flexibility implies higher stiffness leading to higher stresses under a displacement control loading conditions. Therefore, using lower flexibility is considered more conservative under displacement control loading.

In the efforts to reduce the conservatism in the ASME code stress indices, it appears the effect of the flexibility factor was ignored. It is the opinion of the authors of this paper that the stress index and flexibility factor should be treated as a conjugate pair. The reduced secondary stress index should be accompanied with a proper adjustment to the flexibility. To the knowledge of the authors, this aspect was not addressed before and even though some of the published work supported the use of FEA calculated stress indices by experimental verifications, it should be noted that the applicability of these findings are limited to the tested configurations only. The main purpose of this paper is to highlight this issue to the piping analysis

community and further work will be published to propose the required adjustment to the flexibility factor to suit the FEA calculated stress indices.

To explore the relative accuracy of using finite element calculated stress indices along with the ASME Code specified flexibility factors, the following cases are considered for the calculation of the allowable feeder vibration velocity and seismic response for two feeders:

1. Case 1: ANSYS pipe element models with the stress index, C_2 , and flexibility factor, k , based on the ASME code equations.
2. Case 2: ANSYS pipe element models with stress index calculated using the finite element method and flexibility factor based on ASME Code formulas. This is regarded as the current practice adopted by the industry.
3. Case 3: ANSYS pipe elements with stress index calculated using the finite element method and flexibility factor calculated from ASME Code Case N-319-3.
4. Case 4: Using ANSYS shell elements to serve as the reference case (no need for either factor).

FINITE ELEMENT MODELS

Two outlet feeder pipes, A and B, are considered for this paper. Each feeder is made of a lower 2½" pipe and an upper 3" pipe. The feeder modeling is achieved by using the finite element method as implemented in the general-purpose finite element program ANSYS v8.1.9. Figure 1 shows the corresponding finite element models, respectively.

Feeder Geometry

The layout dimensions are per the corresponding design drawings. Each feeder is made of an upper 3" pipe portion and a lower 2½" pipe portion. The nominal dimensions for both sizes of feeder piping are listed in Table 1. The feeders piping models are constructed using ANSYS PIPE16 element with the appropriate stress indices and flexibility factors at locations of bends. The shell models are built using ANSYS SHELL63 elements.

Table 1: CANDU Feeder Piping Dimensions.

| Pipe Size | Outer Diameter (in) | t_{nom} (in) | t_{min} (in) | Inner Diameter (in) |
|-----------|---------------------|----------------|----------------|---------------------|
| 2½" | 3.030 | 0.276 | 0.124 | 2.478 |
| 3" | 3.520 | 0.300 | - | 2.920 |

t_{nom} and t_{min} are the nominal and pressure-based thickness.

Boundary Conditions

The boundary conditions imposed on the finite element models are based on the feeder support information as per the design drawings. Feeders are modeled with all six degrees of freedom constrained at both terminal ends (Grayloc Hub and Header Nozzle). Each feeder has one spring support holding the long upper horizontal piping run. These spring supports are modeled using ANSYS pipe spring element, PSPRING. Upper rigid hangers and lower cantilever supports are modeled by constraining the vertical displacement at each support location.

Material Properties and Model

The feeders are made of SA106 Grade B carbon steel. A linear elastic material model is adopted with Modulus of Elasticity of 29.0×10^6 psi and Poisson's Ratio of 0.3. The density of the piping material and heavy water are 0.0007345 and 0.0000959 lbf.s²/in⁴, respectively. Piping elements allow for the specification of metal and fluid densities required for dynamic analyses. However, with shell or solid models, an equivalent pipe metal density is calculated and used in the finite element shell models.

Secondary Stress Index, C_2

The values of the secondary stress index, C_2 , are calculated based on Section III Division 1 of the ASME BPV code as follows,

$$C_2 = \frac{1.95}{h^3} \geq 1.5, h = t \cdot \frac{R}{r_m^2},$$

where, t is the wall thickness of the pipe bend, R is the bend radius, and r_m is the mean pipe radius.

More specific values of the secondary stress index are obtained using detailed finite element analyses for the specific bend configurations corresponding to both feeders. The secondary stress indices calculated for the feeders considered in this paper are listed in Table 2 for both the nominal and pressure-based thickness.

Flexibility Factor, k

The Flexibility Factors are calculated in accordance with ASME NB-3686.2 2 as follows and are listed in Table 2 for the two feeders considered in this paper:

$$k = \frac{1.65}{h} \cdot \left(\frac{1}{1 + \frac{P \cdot r_m}{t \cdot E} \cdot X_k} \right) \geq 1.0, \text{ and, } X_K = 6 \cdot \left(\frac{r_m}{t} \right)^{\frac{4}{3}} \cdot \left(\frac{R}{r_m} \right)^{\frac{1}{3}},$$

where P is the internal pressure and E is the elastic modulus of the piping material.

ASME Code Case N-319-3 11 provides the following flexibility factors in three perpendicular planes:

$$k_x = 1.0, k_y = \frac{1.25}{h} \cdot \left(\frac{1}{1 + \frac{P \cdot r_m}{t \cdot E} \cdot X_k} \right) \geq 1.0, \text{ and } k_z = \frac{c}{h} \cdot \left(\frac{1}{1 + \frac{P \cdot r_m}{t \cdot E} \cdot X_k} \right) \geq 1.0, \text{ where,}$$

- c Constant that is dependent on the bend/elbow angle, α_0
- =1.65 for $\alpha_0 \geq 180^\circ$
- =1.3 for $\alpha_0 = 90^\circ$
- =1.10 for $\alpha_0 = 45^\circ$
- =1.0 for $\alpha_0 \geq 0^\circ$

$k_x, k_y,$ and k_z are the flexibility factors in the torsion, in-plane bending, and out-of-plane bending, directions respectively. In the analyses considered for this paper, all three values are calculated and the lowest value is used.

Table 2: Stress Indices and Flexibility Factors for CANDU Feeders

| Feeder | Size | Thickness | | C_2 | | k | |
|--------|------|-----------|-------|-------|------|------|------|
| | | (mm) | (in) | ASME | FEM | ASME | CC |
| A | 2½" | 7.01 | 0.281 | 2.59 | 2.43 | 2.47 | 1.81 |
| B | | | | 2.59 | 2.07 | 2.47 | 1.84 |
| A | 2½" | 3.15 | 0.124 | 4.73 | 3.36 | 5.50 | 4.04 |
| B | | | | 4.73 | 2.49 | 5.50 | 4.08 |

CC stands for Code Case N-319-3

For the 2 ½” piping, the bend radius is 4½” for the first two bends in the first feeder and the first bend of the second feeder. All other bends are 15” radius. The first bend tangent angle is 73° 8’ while the second bend tangent angle is 70°.

Finite Element Mesh

The two CANDU feeders analyzed in this paper are shown in Figure 1 with the support systems identified (Header anchor, rigid hanger, spring hanger, seismic damper, lower cantilever support, and end-fitting anchor). ANSYS PIPE16 element is used to model the feeder geometry with the appropriate stress indices and flexibility factors for bends. A total of 2638 nodes and 2637 elements are used for feeder A and 2950 nodes and 2949 elements are used for feeder B. A dense mesh is used on all bends. For the shell models, 12720 nodes and 12672 elements are used for feeder A while 12864 nodes and 12816 elements are used for feeder B. In both shell models ANSYS SHELL43 is used. Figure 2 shows a close-up view for each feeder at the tight radius bend region(s). All pipe and shell models for a feeder are based on the same exact centre line representing the feeder layout.

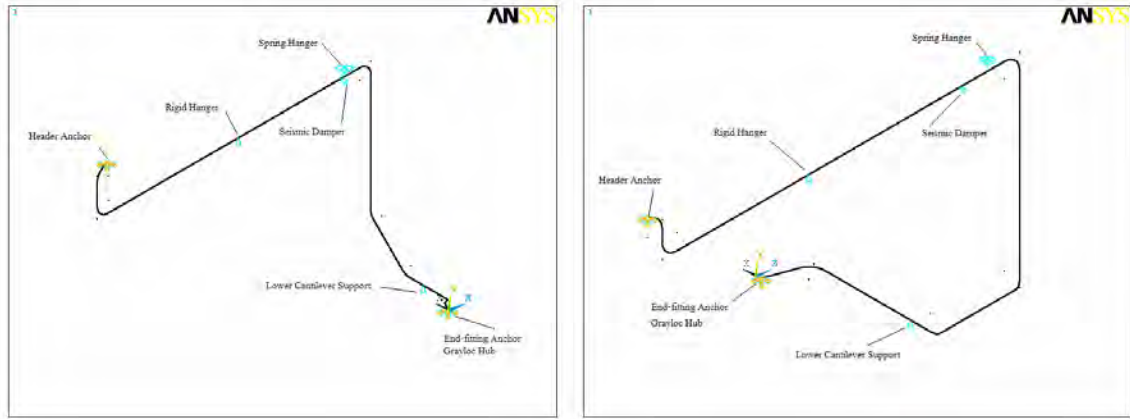


Figure 1: CANDU Reactor Feeders' Models.

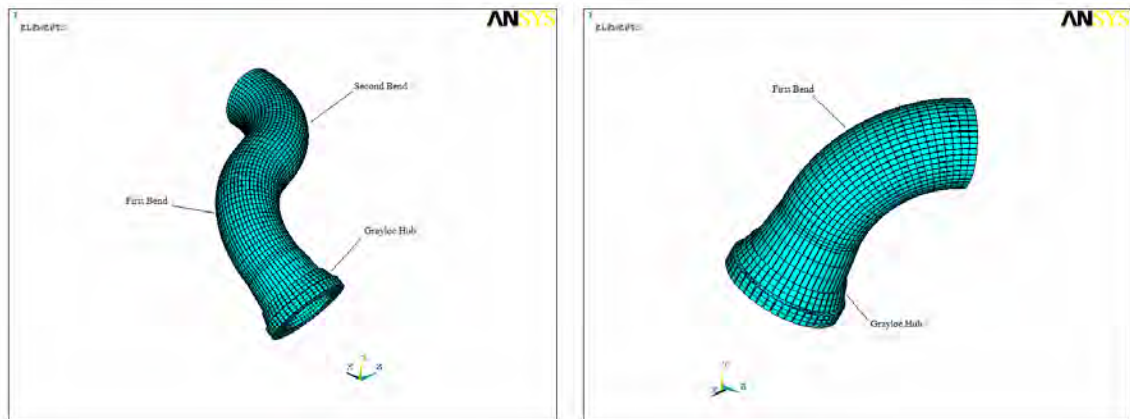


Figure 2: Tight Radius Bend Region & Grayloc Fitting

Vibration Analysis:

It is noted that the finite element results from the shell models are taken as the reference for the piping models. The finite element analysis is performed according to the following procedure:

1. Run Modal Analysis for 0-180 HZ frequency range and obtain the modal frequencies, shapes and stresses.
2. Calculate the allowable vibration velocity for each feeder as follows:

- Determine the natural frequency corresponding to each mode, f_i .
- Determine the highest bending stress, $S_{max,i}$ at the element of maximum stress intensity for each mode.
- Determine the maximum resultant displacement, $d_{max,i}$ for each mode.
- Calculate the maximum velocity for each mode, $V_{max,i}$, as follows:

$$V_{max,i} = \omega_i \cdot d_{max} = 2\pi f_i \cdot d_{max}, \text{ where, } \omega_i \text{ is the natural frequency in radians per second and } f_i \text{ is the natural frequency in cycles per second (Hz)}$$

- Calculate the allowable velocity for each mode, $V_{allowable,i}$, as follows:

$$V_{allowable,i} = \frac{S_{allowable}}{S_{max,i}} \cdot V_{max,i}, \text{ where, } S_{allowable} \text{ is the allowable stress.}$$

- Determine the minimum allowable velocity, $V_{allowable}$,

$$V_{allowable} = \underset{i=1}{\overset{N}{\text{Min}}}(V_{allowable,i}), N \text{ is the number of modes within the 0-180 Hz frequency range.}$$

Seismic Analysis:

The maximum stresses due to Floor Response Spectrum (FRS) and Seismic Anchor Movement (SAM) are calculated for all four cases considered. The multi-point response spectrum analysis feature in ANSYS is used and the SRSS method is adopted to combine the modal responses. Figure 3 shows the end-fitting and outlet header accelerations corresponding to 5% damping. The seismic anchor movements are listed in Table 3.

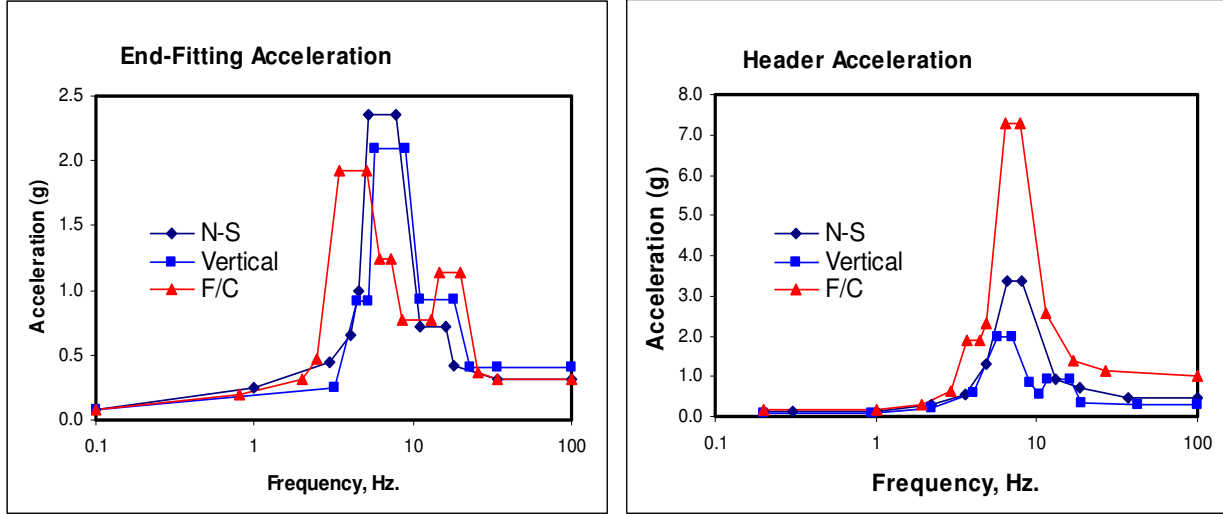


Figure 3: Seismic Accelerations at End-fitting and Outlet Header

Table 3: Seismic Anchor Movements (SAM) at End-fitting

| | X (N-S), (in) | Y (Vertical), (in) | Z (F/C), (in) |
|-------------|---------------|--------------------|---------------|
| End Fitting | 0.078 | 0.069 | 0.133 |
| Header | 0.110 | 0.042 | 0.220 |

N-S: North-South Direction,
F/C: Fuel Channel Direction

FINITE ELEMENT RESULTS

The modal analysis resulted in 34 and 40 natural modes for feeders A and B, respectively, within the 0-180Hz frequency range. Figure 4 shows the allowable modal vibration velocities determined using the nominal thickness for both feeders. Table 4 and Table 5 list the numerical values obtained from the first ten natural modes (for brevity) for feeders A and B, respectively. As observed in Table 4 and Table 5, there is a close agreement between the four cases analyzed with respect to the calculation of the natural frequencies of the two feeder pipes. The last row in each table lists the minimum velocities and is obtained from the full sets of data for each feeder.

As can be seen in Figure 4 and Table 4, the critical mode for feeder A is the fourth mode at 6.6 Hz natural frequency and a corresponding allowable vibration velocity of 234 mm/s (shell model results). At this critical mode, the shell model produces a higher allowable vibration velocity than all three piping models (188, 188, and 189 mm/s). This result alone implies that the use of the FEA calculated secondary stress index is still conservative. However, Figure 4 and Table 4 also show that at other frequencies, using the FEA calculated stress index implies a non-conservative situation where the allowable velocity from the piping models is higher than the shell model (mode 3 for instance). Table 5 shows a similar trend for B. It is observed that the predicted critical mode for feeder A is the same in all four models. This is not the case for feeder B where mode 9 becomes the critical mode when using the piping models. This change in the critical mode highlights the sensitivity of the calculations to the flexibility factor handling using only one value in all planes. It also highlights the different behavior for different bend configurations. It is also observed that the natural frequencies are not significantly sensitive to the flexibility differences. The difference in the calculated allowable velocities is attributed to the differences in the mode shapes.

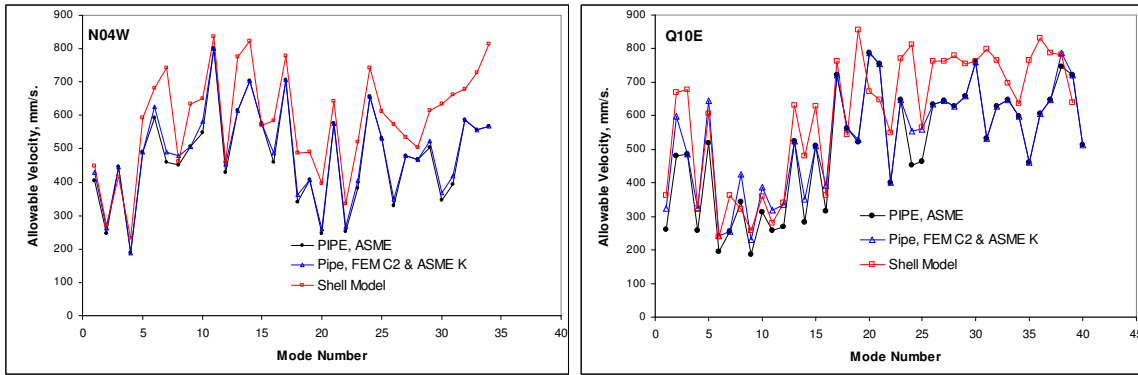


Figure 4: Allowable Vibration Velocity Comparison with t_{nom}

Table 4: FEA Results for CANDU Feeder A with t_{nom}

| Mode | C2&k_ASME | | C2_FEA/k_ASME | | C2_FEA/k_CC | | Shell | |
|----------------|-----------|------------|---------------|------------|-------------|------------|-------|------------|
| | f_i | V_{all} | f_i | V_{all} | f_i | V_{all} | f_i | V_{all} |
| 1 | 3.3 | 403 | 3.3 | 429 | 3.4 | 449 | 3.3 | 449 |
| 2 | 4.3 | 248 | 4.3 | 264 | 4.4 | 244 | 4.3 | 272 |
| 3 | 5.0 | 446 | 5.0 | 446 | 5.0 | 446 | 5.3 | 415 |
| 4 | 6.8 | 188 | 6.8 | 188 | 6.8 | 189 | 6.6 | 234 |
| 5 | 9.8 | 491 | 9.8 | 491 | 9.8 | 491 | 9.7 | 593 |
| 6 | 12.1 | 592 | 12.1 | 626 | 12.1 | 597 | 12.1 | 681 |
| 7 | 13.2 | 460 | 13.2 | 489 | 13.2 | 447 | 13.3 | 742 |
| 8 | 14.7 | 451 | 14.7 | 480 | 14.8 | 412 | 14.7 | 464 |
| 9 | 18.6 | 506 | 18.6 | 506 | 18.6 | 507 | 18.8 | 634 |
| 10 | 20.2 | 549 | 20.2 | 582 | 20.3 | 506 | 20.1 | 652 |
| Minimum | | 188 | | 188 | | 189 | | 234 |

Table 5: FEA Results for CANDU Feeder B with t_{nom}

| Mode | C2&k_ASME | | C2_FEA/k_ASME | | C2_FEA/k_CC | | Shell | |
|----------------|-----------|------------|---------------|------------|-------------|------------|-------|------------|
| | f_i | V_{all} | f_i | V_{all} | f_i | V_{all} | f_i | V_{all} |
| 1 | 1.9 | 259 | 1.9 | 323 | 1.9 | 316 | 1.9 | 363 |
| 2 | 3.0 | 479 | 3.0 | 597 | 3.0 | 577 | 3.1 | 668 |
| 3 | 4.6 | 485 | 4.6 | 485 | 4.6 | 485 | 4.6 | 678 |
| 4 | 6.3 | 259 | 6.3 | 323 | 6.4 | 318 | 6.7 | 325 |
| 5 | 8.1 | 519 | 8.1 | 644 | 8.1 | 618 | 8.2 | 606 |
| 6 | 9.9 | 195 | 9.9 | 241 | 9.9 | 233 | 9.7 | 240 |
| 7 | 12.2 | 255 | 12.2 | 255 | 12.2 | 270 | 11.9 | 363 |
| 8 | 13.7 | 344 | 13.7 | 425 | 13.8 | 406 | 13.7 | 322 |
| 9 | 14.8 | 186 | 14.8 | 230 | 15.0 | 204 | 14.9 | 257 |
| 10 | 18.2 | 313 | 18.2 | 386 | 18.2 | 351 | 17.9 | 359 |
| Minimum | | 186 | | 230 | | 204 | | 240 |

f_i is the natural frequency corresponding to the controlling mode shape, Hz.
 V_{all} is the allowable vibration velocity, mm/s.

Figure 5 demonstrates the allowable vibration velocity results when using the pressure-based thickness at the tight radius bends region. Table 6 and Table 7 list the numerical values corresponding to the first 10 modes of Figure 5. Again, it is evident that the allowable vibration velocities obtained from the piping models with FEA calculated stress index are not conservative (higher allowable compared to the shell model). Using the ASME code case flexibility helps improve the accuracy of the allowable velocity; however, results are still non-conservative to some extent.

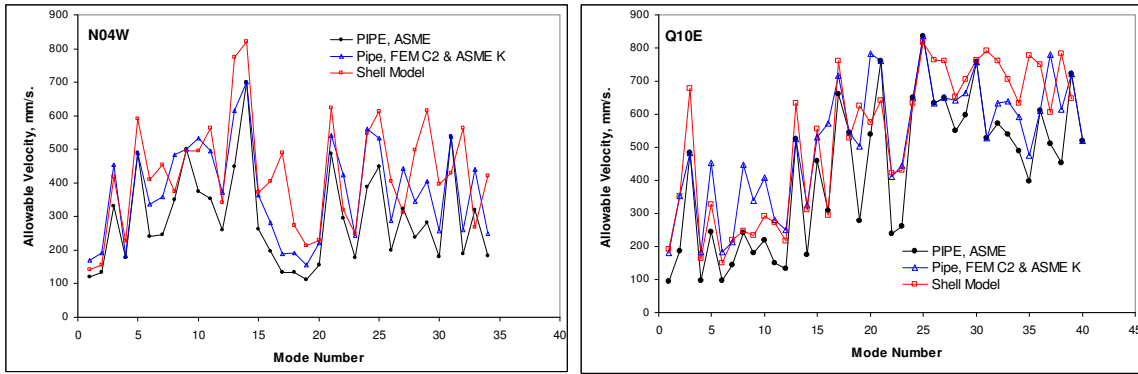


Figure 5: Allowable Vibration Velocity Comparison with t_{min}

Table 6: FEA Results for CANDU Feeder A with t_{min}

| Mode No. | C2&k_ASME | | C2_FEA/k_ASME | | C2_FEA/k_CC | | Shell | |
|----------------|-----------|----------------|---------------|----------------|-------------|----------------|----------|----------------|
| | f_i Hz | V_{all} mm/s | f_i Hz | V_{all} mm/s | f_i Hz | V_{all} mm/s | f_i Hz | V_{all} mm/s |
| 1 | 3.1 | 119 | 3.1 | 168 | 3.2 | 145 | 3.2 | 142 |
| 2 | 3.8 | 134 | 3.8 | 190 | 3.9 | 161 | 3.9 | 155 |
| 3 | 5.0 | 330 | 5.0 | 453 | 5.0 | 424 | 5.3 | 419 |
| 4 | 6.6 | 177 | 6.6 | 184 | 6.6 | 185 | 6.4 | 226 |
| 5 | 9.8 | 491 | 9.8 | 491 | 9.8 | 491 | 9.7 | 592 |
| 6 | 11.9 | 241 | 11.9 | 336 | 11.9 | 311 | 12.0 | 410 |
| 7 | 12.8 | 247 | 12.8 | 358 | 12.9 | 313 | 13.2 | 455 |
| 8 | 14.3 | 349 | 14.3 | 485 | 14.4 | 398 | 14.3 | 376 |
| 9 | 18.5 | 500 | 18.5 | 500 | 18.5 | 501 | 18.7 | 495 |
| 10 | 19.9 | 374 | 19.9 | 533 | 19.9 | 456 | 19.8 | 496 |
| Minimum | | 112 | | 155 | | 145 | | 142 |

Table 7: FEA Results for CANDU Feeder B with t_{min}

| Mode No. | C2&k_ASME | | C2_FEA/k_ASME | | C2_FEA/k_CC | | Shell | |
|----------------|-----------|----------------|---------------|----------------|-------------|----------------|----------|----------------|
| | f_i Hz | V_{all} mm/s | f_i Hz | V_{all} Mm/s | f_i Hz | V_{all} mm/s | f_i Hz | V_{all} mm/s |
| 1 | 1.7 | 95 | 1.7 | 180 | 1.8 | 168 | 1.8 | 191 |
| 2 | 3.0 | 186 | 3.0 | 352 | 3.0 | 326 | 3.1 | 352 |
| 3 | 4.6 | 484 | 4.6 | 484 | 4.6 | 484 | 4.6 | 677 |
| 4 | 5.8 | 97 | 5.8 | 184 | 5.9 | 168 | 6.3 | 165 |
| 5 | 7.9 | 244 | 7.9 | 453 | 8.0 | 395 | 8.1 | 327 |
| 6 | 9.3 | 98 | 9.3 | 183 | 9.4 | 151 | 9.4 | 149 |
| 7 | 11.8 | 145 | 11.8 | 214 | 11.9 | 213 | 11.7 | 221 |
| 8 | 13.3 | 243 | 13.3 | 447 | 13.4 | 350 | 13.3 | 247 |
| 9 | 14.2 | 181 | 14.2 | 340 | 14.3 | 257 | 14.5 | 235 |
| 10 | 17.7 | 220 | 17.7 | 408 | 17.8 | 338 | 17.6 | 290 |
| Minimum | | 95 | | 180 | | 151 | | 149 |

With regard to the results from the seismic analyses, Table 8 and Table 9 list the maximum displacements and stresses for both feeders with nominal and pressure-based thickness. At the nominal thickness, the differences in the predicted maximum values are small and the stresses are slightly non-conservative when using the FEA calculated stress index paired with the ASME flexibility factor. The calculated maximum stress gets closer to the shell model value by using the Code Case flexibility factor. The differences are magnified when using the pressure-based thickness. The calculated maximum stress due to the seismic load is 54.4 ksi and 53.4 ksi for feeders A and B, respectively.

Table 8: Seismic Analysis Results for CANDU Feeders with t_{nom}

| Feeder | C2&k_ASME | | C2_FEA/k_ASME | | C2_FEA/k_CC | | Shell | |
|--------|-----------|------------|---------------|------------|-------------|------------|-----------|------------|
| | D_{max} | S_{max} | D_{max} | S_{max} | D_{max} | S_{max} | D_{max} | S_{max} |
| | In | 10^3 psi | In | 10^3 psi | in | 10^3 psi | in | 10^3 psi |
| A | 1.646 | 42.4 | 1.646 | 39.9 | 1.641 | 43.9 | 1.774 | 38.6 |
| B | 1.215 | 35.0 | 1.215 | 28.0 | 1.238 | 29.5 | 1.171 | 30.1 |

D_{max} is the maximum displacement from the whole model

S_{max} is the maximum stress intensity in the tight radius region

Table 9: Seismic Analysis Results for CANDU Feeders with t_{min}

| Feeder | C2&k_ASME | | C2_FEA/k_ASME | | C2_FEA/k_CC | | Shell | |
|--------|-----------|------------|---------------|------------|-------------|------------|-----------|------------|
| | D_{max} | S_{max} | D_{max} | S_{max} | D_{max} | S_{max} | D_{max} | S_{max} |
| | In | 10^3 psi | In | 10^3 psi | in | 10^3 psi | in | 10^3 psi |
| A | 1.641 | 70.3 | 1.644 | 49.9 | 1.616 | 58.6 | 1.670 | 54.4 |
| B | 1.115 | 67.6 | 1.116 | 36.5 | 1.122 | 42.8 | 1.140 | 53.4 |

The results presented show that the use of the ASME code stress index and flexibility factor pair is conservative providing lower allowable vibration velocity and higher seismic stresses. More significant effects of the C_2 and k pair are observed when using the pressure-based thickness locally at the tight radius bends.

CONCLUSIONS

The finite element method is adapted to model two feeder pipes using 3D pipe and shell finite elements. Two thickness values at the tight radius bends are used; nominal and pressure-based. Two types of analyses were performed on the pipe and shell FE models. The response parameters used for the comparison between different models are the allowable modal vibration velocity and the maximum stress intensity due to seismic loading. The results of the comparisons show that the piping model with FEA calculated secondary stress index without correcting the flexibility factor is not conservative in comparison to a shell model. The results also show that correcting the flexibility factor using the ASME Code Case N-319-3 improves the results; however they are still not conservative. Using the ASME code stress index and flexibility factor is generally conservative. More analyses are needed to explore the response from different feeder piping with different tight radius bend configurations. Detailed thinning profiles using Shell and/or Solid FEA models should be evaluated. The piping models may benefit from a better formulation of the underlying beam elements by introducing a more appropriate flexibility effects by using a proper flexibility matrix with input representing more than one plane.

REFERENCES

- Standards and Guides for Operation and Maintenance of Nuclear Power Plants, ASME OM-S/G-2003.
- ASME Boiler and Pressure Vessel Code, Section III, "Rules for Construction of Nuclear Power Plants", 2004.
- Vernon C. Matzen and Ying Tan, "The History of the B2 Stress Index", Transactions of the ASME, Journal of Pressure Vessel Technology, Vol 124, pp. 168-16, 2002.
- S.Y. Eom, U. Abdelsalam, D.K. Vijay, "Calculation of Piping Weld Stress Indices using 3D FE Analysis", Second Canadian Workshop on Engineering Structural Integrity, CWESI-2, Canadian Nuclear Society, Design and Materials Division, Toronto, Ontario, Canada, April 3-4, 2006.
- Ying Tan, Vernon C. Matzen, and Xi Yuan, "A Margin-Consistent Procedure for Calculating the B2 Stress Index and A Proposed New Design Equation", SMiRT 16, Washington DC, August 2001.
- Vernon C. Matzen and Ying Tan, "Using Finite Element Analysis to Determine Piping Elbow Bending Moment (B2) Stress Indices", WRC Bulletin 42, June 2002.
- R. Kumar and M.A. Saleem, "Bend Angle Effect on B₂ and C₂ Stress Indices for Piping Elbows", Journal of Pressure Vessel Technology, May 2001, Vol 123, PP. 226-231.
- R. Kumar and M. Saleem, "B₂ and C₂ Stress Indices for Large-Angle Bends", Journal of Pressure Vessel Technology, May 2002, Vol. 124, PP. 177-1876.
- ANSYS v8.1 User's Manual.
- Lixin Yu, and Vernon C. Matzen, "B2 Stress Index for Elbow Analysis", Nuclear Engineering and Design 192 (1999) 261-270.
- CASES OF ASME BOILER AND PRESSURE VESSEL CODE, Case N-319-3, Approval Date: January 1, 2000.